Rearrangement of energy bands : Quantum, semi-quantum, and classical models

UMR CNRS 8101, Université du Littoral, Dunkerque, FRANCE
email: zhilin@univ-littoral.fr

B. ZHILINSKII

1 Introduction

This is a short summary of my talk given in IRMA, Strasbourg, in which I presented an overview of qualitative approach to the description of quantum finite-particle systemes, typically atoms and molecules.

The qualitative analysis of highly excited atomic and molecular systems was developped and applied to real molecular systems during last 10-15 years mainly by the author of the present talk in collaboration with many different scientists working in different domains: Dr. D. Sadovskii, G. Dhont, Ch. VanHaeke L. Grondin (Dunkerque); Dr. V. Boudon (Dijon); Dr. F. Faure (Grenoble); Prof. M. Herman, M.I. El Idrissi (Brussels); Prof. L. Michel (late), (IHES); Dr. I. Kozin (Warwick, UK); Prof S. Brodersen, (Århus, Danemark); Dr. R. Cushman (Utrecht); Dr. I. Pavlichenkov, S. Petrov (Moscow).

There exist several recent reviews on the subject [1–5] which cover the formal basic tools needed for the qualitative analysis, like theory of invariants, Morse theory, orbifold construction, generating function formalism, etc, and concrete molecular applications to rotational, vibrational and electronic structure of molecules. The basic idea of the qualitative approach is the simultaneous use of classical and quantum description. In order to analyse the qualitative features of effective quantum Hamiltonians which are largely used to describe molecular systems, the corresponding classical symbol is introduced and analysed in the spirit of qualitative topological theory of dynamical systems. The correspondence between qualitative features of classical system and its quantum prototype is served to characterize quantum systems.

Very often only part of dynamical variables is considered as purely classical ones. Another part of dynamical variables remains to be quantum. We refer to such approach as semi-quantum description. The analysis of the same problem within purely quantum, semi-quantum and completely classical way enables us to understand better qualitative features of molecular quantum problems.

One of the most clearly seen qualitative features of the typical system of molecular energy levels is the presence of so-called bands or branches. An isolated band has internal structure which can be described by classical mechanics whereas its existence is due to the presence of one quantum state with respect to another group of dynamical variables. From the molecular point of view such separation of variables into "classical" and "quantum" can be associated with splitting into "slow" (classical) and "fast" (quantum) variables. Rotational structure of isolated vibrational state or vibrational structure of vibrational polyads for isolated electronic state are typical examples.

As soon as energy bands exist, two rather different natural qualitative questions can be formulated.

i) What is the qualitative internal structure of isolated bands?

ii) Can we distinguish bands by some labels and to formulate some rules for rearrangement of bands under modification of some physical characteristics, for example under the variation of a strict or approxiamte integral of motion?

The answer to the first question is mainly based on the analysis of the classical limit for effective quantum Hamiltonian describing the internal structure of isolated energy bands. The topology of the effective classical phase space and the action of the symmetry group on it together with equivariant Morse theory enables one to classify and to characterize many important qualitative features of quantum systems which are related in the classical limit with the classical bifurcations.

Typical classical phase spaces for effective molecular Hamiltonians are:

i) Effective rotational Hamiltonian - two dimensional sphere, S_2.

ii) Effective Hamiltonian for vibrational polyads formed by N degenerate vibrations - complex projective space, CP_{N-1}.

iii) Effective Hamiltonian for internal structure of Rydberg n-shells of atoms and molecules - direct product of two two-dimensional spheres, $S_2 \times S_2$.

Qualitative features of quantum energy levels within an isolated energy band in the presence of different invariance symmetry groups were studied in many papers. We refer, for example, to [5–11] for rotational problems, to [12–15] for internal structure of vibrational polyads, to [3,16,17] for internal structure of Rydberg multiplets. Energy level clustering and modification of the cluster structure under variation of control parameters (the so called quantum bifurcations) are the most essential qualitative features of the internal structure of isolated energy bands.

The characterization of the energy band as a whole is another very important qualitative aspect of the quantum energy level system. Probably the simplest global characterization of a band in a quantum formalism can be done by the number of quantum states in the band. The method of counting the number of states using the generating function approach (Molien or Poincaré series) was suggested in [18]. Discovered later [1,2,19–21] expression

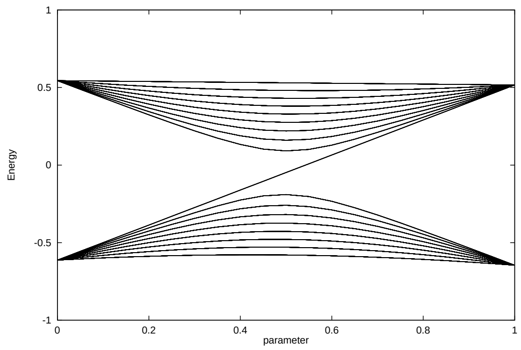

Fig. 1. Energy level spectrum of the model Hamiltonian (1) with $S = 1/2$, $J = 4$.

for the numbers of states in terms of Todd polynomials for effective classical phase space and Chern classes for vector bundles (introduced for energy bands within the semi-quantum approach) suggests very interesting relation with general index formulae for the deformation quantization [22,23].

2 Monodromy and redistribution

The redistribution of energy levels between bands under the variation of some integral of motion was initially recognized as a universal phenomena in [24]. Very simple model which shows the redistribution of one level between two bands in the energy spectrum under the variation of one parameter was formulated in terms of two coupled angalar momenta. Namely the Hamiltonian has the form

$$H = (1 - t)S_z + t(\mathbf{J} \cdot \mathbf{S}), \tag{1}$$

where $\mathbf{S} = (S_x, S_y, S_z)$ is the spin operator with $S = 1/2$, $\mathbf{J}$ is the angular momentum with sufficiently high J. The limit $t = 0$ corresponds to two bands with the same numbers of states, $2J+1$. $t = 1$ limit corresponds to two bands which have different number of states, $2J + 2$ and $2J$ (see Figure 1).

Generalization of this model to higher S values leads to an interesting relation with the monodromy phenomenon [25–28]. It

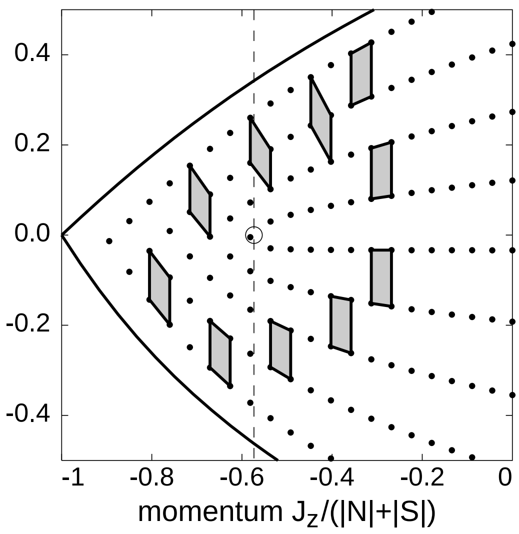

Fig. 2. Monodromy map [29].

was shown in [29] that the Hamiltonian (1) in classical limit and in certain region of parameter values t has classical monodromy. The classical monodromy for this completely integrable classical problem is related to the presence of an isolated singular point on the energy momentum map. The manifestation of this classical monodromy in the corresponding quantum spectrum can be visualized easily with the aid of motion of the elementary cell around the singularity (see Figure 2).

If we look at Figure 2 from the point of view of regular lattice of points we can associate the singularity responcible for the monodromy with the defect of this 2-dimensional lattice. The analogy is rather formal but it leads immediately to the question about existence of “inverse” defect. To explain what is meant by “inverse” defect let first remark that the number of points at each J_z value, which is grater than the singular value, remains constant. At the same time the number of states at lower (with respect to the singularity) J_z values decreases linearly with J_z. Other examples of monodromy in quantum problem (see for example [30] where the monodromy for the hydrogen atom in fields was found) lead to another values of the monodromy but the slope for the number of states function in the neighbourhood of the singularity point remains convex. At the same time for the abstract

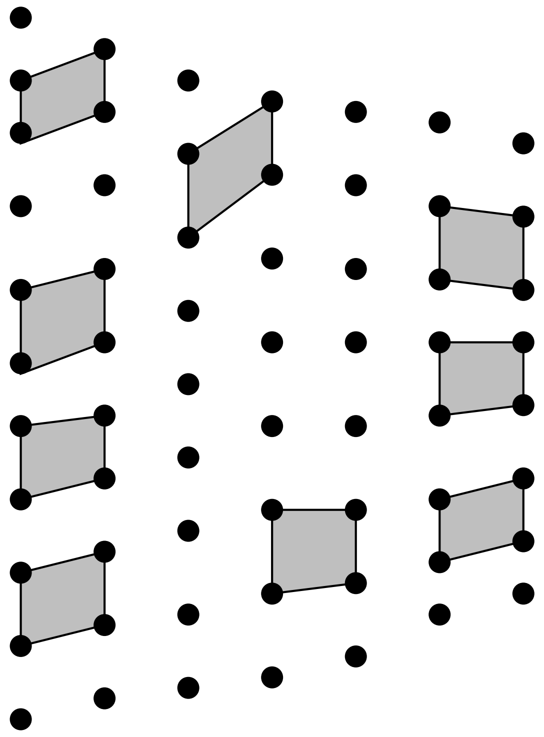

Fig. 3. “Inversed” defect of quantum-state-lattice.

lattice it is quite easy to construct defect which correspond to concave behaviour of the number-of-state function in the neighbourhood of the defect.

An example of such formal lattice with defect is given in Figure 3. I will name such defect “inversed”. It is not clear for me if such a defect can exist in the case of the lattice of quantum states. It is quite possible that the restriction to the existence of such kind of defects for Hamiltonian dynamical systems is due to the convexity property of the energy-momentum map. But even if this is the case, more general question arises. What kind of systems can be associated with such symmetry (I do not want to add “mirror”) transformation of the lattice with defect.

3 Monodromy line for system with three degrees of freedom

This section is mainly based on the commun work with L. Grondin and D. Sadovskii [31]. To see the possible generalization of the redistribution effect to systems with higher number of degrees of freedom let now consider one particular example of a system formed by three coupled angular momenta $\mathbf{L}_1$, $\mathbf{L}_2$, and $\mathbf{L}_3$ in the presence of the SO(3) symmetry [31]. Due to the SO(3) invariance our system has two integrals of motion, the amplitude J of the total angular momentum $\mathbf{J} = \mathbf{L}_1 + \mathbf{L}_2 + \mathbf{L}_3$ and one of the components of $\mathbf{J}$.

To describe unambiguously a system of three vectors in the presence of the SO(3) symmetry, i.e., to specify a configuration of these vectors up to any rotation of the coordinate frame around the origin, we can use three scalar products $\tilde{X}_k = (\mathbf{L}_i \cdot \mathbf{L}_j)$, where (ijk) is a cyclic permutation of (123), and the mixed product $\tilde{Y} = (\mathbf{L}_1 \cdot [\mathbf{L}_2 \wedge \mathbf{L}_3])$ respectively [32]. If we extend the SO(3) symmetry by adding as symmetry operation the simultaneous inversion of the vectors, the mixed product Y is no longer necessary since "left" and "right" orientations become equivalent. In the case of ordinary vectors the additional symmetry operation is 3-space inversion and the resulting group is O(3), in the case of angular momenta (which are invariant with regard to spatial inversion) this operation is time reversal $\mathcal{T}$ and the group SO(3)$\times\mathcal{T}$ is isomorphic to O(3).

It follows that an arbitrary SO(3) invariant Hamiltonian can be written as a polynomial expansion in terms of $\tilde{X}_1$, $\tilde{X}_2$, and $\tilde{X}_3$, and Y, and in the case of the extended symmetry SO(3) $\times\,\mathcal{T}$ the Hamiltonian does not depend on $\tilde{Y}$ which changes sign under the time reversal. One simple example of a one-parameter family of Hamiltonians is extremely interesting from the point of view of comparison with initial problem (1).

$$H_\alpha = \alpha(\mathbf{L}_1 \cdot \mathbf{L}_2) + (1-\alpha)(\mathbf{L}_1 \cdot \mathbf{L}_3). \tag{2}$$

This family describes recoupling of three angular momenta which is often present in various physical systems. Thus in atoms, where spin and angular momentum of the electron(s) are coupled to the spin of the nucleus, the two limits of (2) with $\alpha = 0$ and $\alpha = 1$ represent two different Hund's coupling cases. Many other examples can be easily drawn from molecular physics. The quantum spectrum of the system with three coupled angular momenta can be computed straightforwardly. For given fixed amplitudes $|\mathbf{L}_1|$, $|\mathbf{L}_2|$, and $|\mathbf{L}_3|$, dimension of the space of quantum wave functions equals $(2l_1+1)(2l_2+1)(2l_3+1)$, where l_1, l_2, and l_3 are respective quantum numbers. Each quantum state can also be chosen as an eigenstate of operators $\mathbf{J}$ and J_z which correspond to the two strict integrals of motion in the presence of the SO(3) symmetry. The $2j+1$ states with the same quantum number j and different projections j_z are degenerate. We call the group of degenerate levels with the same j a j-band. Such j-bands can be in turn assembled into "superbands". Existence and structure of superbands naturally depends on the Hamiltonian.

In the case of the Hamiltonian (2) the superbands are associated with additional approximate (or "good") quantum numbers. If α in (2) is close to zero the amplitude of the angular momentum $\mathbf{J}_{13} = \mathbf{L}_1 + \mathbf{L}_3$ is nearly conserved and j_{13} serves as a good quantum number. Otherwise, when α in (2) is close to 1, the quantum number j_{12} of the angular momentum $\mathbf{J}_{12} = \mathbf{L}_1 + \mathbf{L}_2$ is a good quantum number. We can further simplify the situation by assuming that the amplitude of one of the momenta, say $\mathbf{L}_1$, is much smaller than that of two others and also smaller than the module of their difference:

$$l_1 < l_2, \quad l_1 < l_3, \quad l_1 < |l_2 - l_3|.$$

In this case the spectrum of the Hamiltonian (2) in both limits $\alpha \approx 0$ and $\alpha \approx 1$ consists of $2l_1+1$ "super-bands" formed by a number of degenerate j-bands. The number of superbands in two limiting cases is the same, $2l_1+1$, but the number of bands within each superband is different.

In the example of the quantum energy level spectrum of H_α shown in fig. 4 (left), l_1 equals $\frac{1}{2}$ and we can see two superbands. At small α these superbands are characterized by quantum numbers

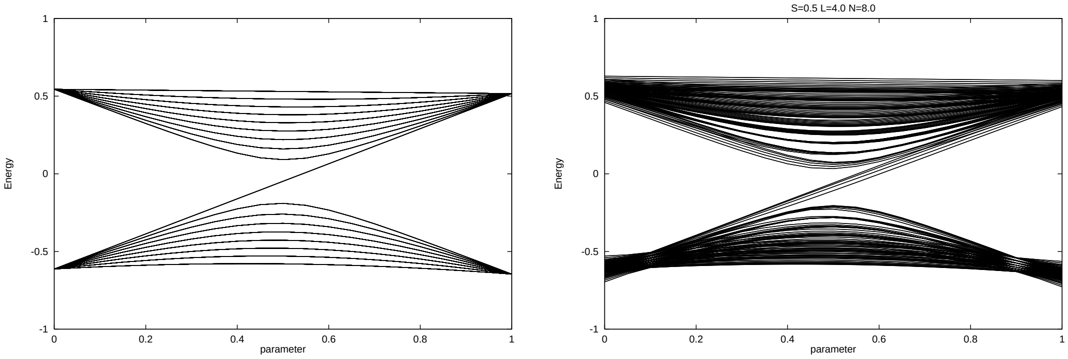

Fig. 4. Energy level spectrum of the model Hamiltonian (2) with $L_1 = 1/2$, $L_2 = 4$, and $L_3 = 8$ (left) and of the same model but with with additional small perturbation which breaks $SO(3)$ symmetry. The degeneracy within the bands is removed but the J bands are still grouped into two superbands.

$j_{13} = 7.5$ and $j_{13} = 8.5$ while at large $\alpha \approx 1$ we use $j_{12} = 3.5$ and $j_{12} = 5.5$. In the limit $\alpha \approx 0$ each superband includes nine j-bands with $j_{13} - l_2 \leq j \leq j_{13} + l_2$. For α close to 1, the two superbands consist of different number of j-bands with $l_3 - j_{12} \leq j \leq j_{12} + l_3$.

Comparing fig. 4, left, to similar figure 1 convinces immediately that the above analysis of recoupling of three angular momenta in the presence of the SO(3) symmetry is very similar to the analysis of coupling of two angular momenta in the presence of the SO(2) symmetry. The main difference is that instead of redistribution of a single energy level (or a group of a fixed number of levels) between j-bands we observe redistribution of j-bands between superbands. To see this latter phenomenon more clearly it is sufficient to break slightly the SO(3) symmetry as shown in fig. 4, right. Symmetry breaking removes the strict degeneracy of levels within each j-band but redistribution of bands persists because it is a topologically stable phenomenon.

From the fully classical point of view the Hamiltonian (2) has three degrees of freedom and two first integrals J and J_z imposed by the continuous symmetry $SO(3)$. This system is, therefore, Liouville integrable. The phase space is the direct product of three spheres $S_2 \times S_2 \times S_2$. The values of L_1, L_2, and L_3, define the radii of the 2-spheres and the range of possible values of J. All regular dynamically invariant subspaces of this phase space are 3-tori. The values L_1, L_2, and L_3 play the role of additional parameters which give raise to a great variety of systems with different dynamically invariant singular subspaces.

To describe the action of the symmetry group SO(3) on $S_2 \times S_2 \times S_2$ for all possible (nonzero) values of L_1, L_2, and L_3 we use normalized principal invariant polynomials $X_k = \tilde{X}_k (L_i L_j)^{-1}$,

$$X_1 = \frac{\mathbf{L}_2 \cdot \mathbf{L}_3}{L_2 L_3}, \quad X_2 = \frac{\mathbf{L}_3 \cdot \mathbf{L}_1}{L_3 L_1}, \quad X_3 = \frac{\mathbf{L}_1 \cdot \mathbf{L}_2}{L_1 L_2},$$

and the auxiliary polynomial

$$Y = \tilde{Y} \, (L_1 L_2 L_3)^{-1} = \mathbf{L}_1 \cdot (\mathbf{L}_2 \wedge \mathbf{L}_3) \, (L_1 L_2 L_3)^{-1},$$

which depends algebraically on the X's,

$$\begin{aligned} Y^2 &= \det \begin{pmatrix} (\mathbf{L}_1 \cdot \mathbf{L}_1) & (\mathbf{L}_1 \cdot \mathbf{L}_2) & (\mathbf{L}_1 \cdot \mathbf{L}_3) \\ (\mathbf{L}_2 \cdot \mathbf{L}_1) & (\mathbf{L}_2 \cdot \mathbf{L}_2) & (\mathbf{L}_2 \cdot \mathbf{L}_3) \\ (\mathbf{L}_3 \cdot \mathbf{L}_1) & (\mathbf{L}_3 \cdot \mathbf{L}_2) & (\mathbf{L}_3 \cdot \mathbf{L}_3) \end{pmatrix} (L_1 L_2 L_3)^{-2} \\ &= 1 + 2X_1 X_2 X_3 - X_1^2 - X_2^2 - X_3^2. \end{aligned}$$

Each orbit of the $SO(3)$ action is characterized by (x_1, x_2, x_3), the values of X_1, X_2, and X_3, and the sign of y, the value of Y, and represents uniquely a configuration of the vector triplet $(\mathbf{L}_1, \mathbf{L}_2, \mathbf{L}_3)$. For all regular configurations the value of Y is nonzero, it vanishes for all planar and collinear configurations. If we go to a larger group $SO(3) \times \mathcal{T}$ then two regular orbits of the $SO(3)$ action with the same $|y| \neq 0$ simply become one orbit of the $SO(3) \times \mathcal{T}$ action.

The space of all orbits of the $SO(3) \times \mathcal{T}$ action or the *orbifold* can be constructed in the ambient space R_3 with coordinates (x_1, x_2, x_3). Orbits with $y = 0$ lie on a closed surface which is defined in this space by equation $Y^2 = 0$. As shown in 5 this pillow-like surface can be described as a blown up tetrahedron with four

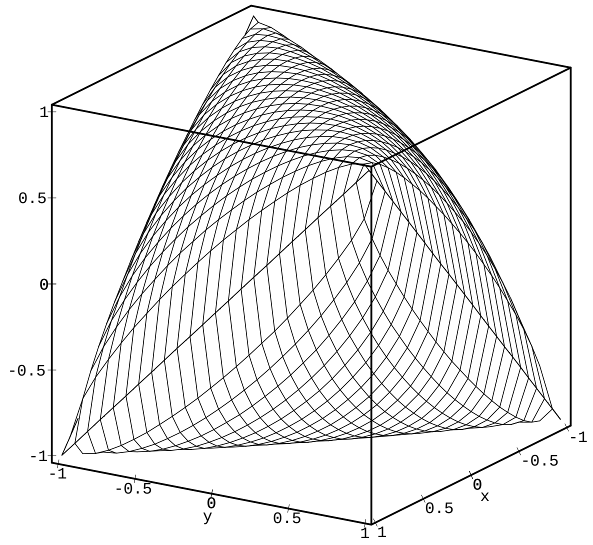

Fig. 5. Orbit space of the $SO(3) \times \mathcal{T}$ group action parametrized by the values of three normalized scalar products.

Table 1
Inverse image of points of the orbifold in the case of $SO(3) \times \mathcal{T}$ and $SO(2) \times Z_2$ group actions on $S_2 \times S_2 \times S_2$ and $S_2 \times S_2$ respectively.

points of orbifold	image in $S_2 \times S_2 \times S_2$	image in $S_2 \times S_2$
vertices	sphere S_2	point
surface	real projective space RP_3	circle S_1
interior	disjoint union of *two* RP_3	disjoint union of *two* S_1

singular vertices and smooth edges. The vertices correspond, of course, to the four collinear configurations of $(\mathbf{L}_1, \mathbf{L}_2, \mathbf{L}_3)$. All regular orbits lie inside the surface. The orbifold has the topology of a closed ball with four singular points.

Geometrically the orbit space of the $SO(3) \times \mathcal{T}$ group action on $S_2 \times S_2 \times S_2$ is the same as the space of orbits of the $SO(2) \times Z_2$ group action on $S_2 \times S_2$. (Note that in [3] invariants (X_1, X_2, X_3), K, and Y correspond to (S_z, N_z, ξ), J_z, and σ.) The stabilizers of orbits are, of course, larger in the case of $SO(3)$ than in the case of $SO(2)$. To learn more on the similarity and difference between the $SO(2)$ invariant system with two angular momenta and the $SO(3)$ invariant system with three angular momenta it is instructive to compare the orbits of the two group actions presented in Table 1.

Table 2
Possible singular planar sections V_k of the orbit space $\mathcal{O}$ for the $SO(3)$ symmetric system with three angular momenta.

notation	topology of singular section	
g	generic point on the surface $(y = 0)$ of $\mathcal{O}$	$\circ$
s	singular point, one of the vertices of $\mathcal{O}$	$\bullet$
r	line on the surface of $\mathcal{O}$ connecting two vertices	$\bullet\!\!-\!\!\!-\!\!\bullet$
1	closed disk with one singular point on the border	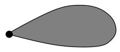
2	closed disk with two singular points on the border	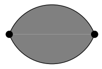
3	closed disk with three singular points on the border	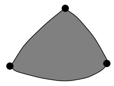

All regular sections V_k have a topology of a closed disc with border S_1. This topology does not change if the variation of k is sufficiently small. Corresponding regular reduced spaces are diffeomorphic to a 2-sphere S_2. Topology of singular sections V_k is summarized in Table 2. In the case of the singular section s, we can introduce more fine classification by denoting by s^* those particular sections which are at the same time tangent to the orbifold.

The ratio $l_1{:}l_2{:}l_3$ defines orientation of the constant level plane of K, which in turn defines entirely a whole continuous family of sections V_k and the corresponding family of reduced spaces. The parameter space of all possible $l_1{:}l_2{:}l_3$ can be represented as an equilateral triangle shown in Figure 6. Let suppose that $l_i \neq 0$. The vertices, sides, and interior points of this trinagle correspond to configurations with two, one, and zero momenta are respectively infinite. Each point of this parameter space represents a family of sections V_k. We can also always choose $0 < l_1 \leq l_2 \leq l_3$. This means that it is sufficient to characterize only points which belong to the small triangle AOD shown in Figure 6.

All families of sets of singular sections which appear for all possible values of J^2 in a problem with fixed ratio of angular momenta modulus are listed in Table 3. It is important that the set of singular sections is independent of the form of the Hamiltonian

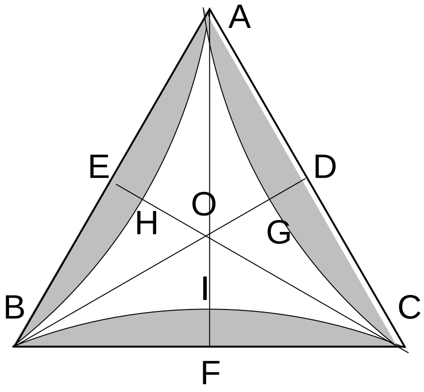

Fig. 6. Regions corresponding to different ratio of angular momenta leading to qualitatively different sets of singular sections.

Table 3
Possible families of planar sections V_k of the orbit space for the $SO(3)$ symmetric system with three angular momenta. Only regions with $0 < l_1 \le l_2 \le l_3$ are listed. By s^* we denote the specific section at singular point which is tangent to the cone at s.

region in 6	l_1:l_2:l_3	family
O	$0 < l_1 = l_2 = l_3$	$g3s$
A	$0 < l_1, \quad l_2 = \infty, \quad l_3 = \infty$	rr
D	$0 < l_1 = l_2, \quad l_3 = \infty$	$s2s$
G	$0 < l_1 = l_2, \quad l_3 = l_1 + l_2$	s^*2s
AD	$0 < l_1 < l_2, \quad l_3 = \infty$	$s11s$
DG	$0 < l_1 = l_2 < l_3/2 < \infty$	$s2s$
OG	$0 < l_1 = l_2 < l_3 < 2l_1$	$g12s$
AO	$0 < l_1 < l_2 = l_3$	$g21s$
AG	$0 < l_1 < l_2, \quad l_3 = l_1 + l_2$	s^*11s
AGD	$0 < l_1 < l_2, \quad l_1 + l_2 < l_3 < \infty$	$s11s$
AOG	$0 < l_1 < l_2 < l_3 < l_1 + l_2$	$g111s$

(assuming, surely, that it is invariant with respect to the same symmetry group).

Set of singular sections of the type $s11s$ corresponds to the set of sections studied in [29] on the example of more simple problem.

To see better the presence of singular sections for problems with different ratio $l_1 : l_2 : l_3$ and modification of the set of singular

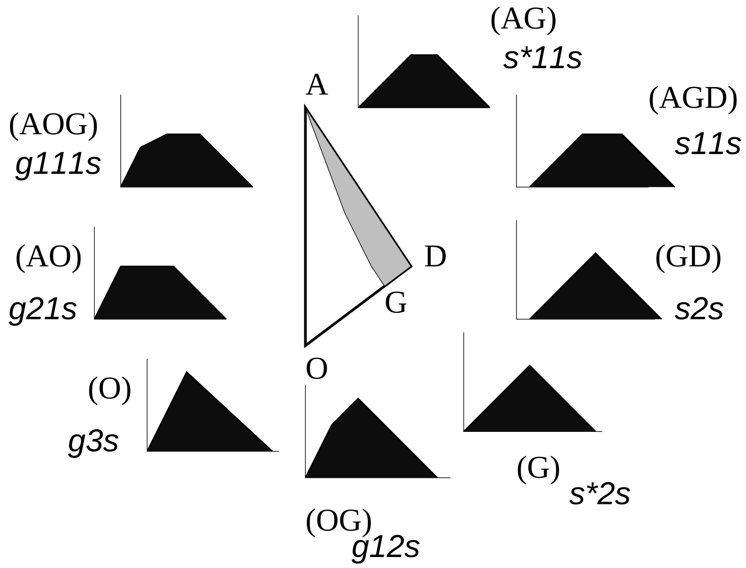

Fig. 7. Density of states as a function of the total angular momentum for different ratio of three coupled angular momenta.

sections along with the variation of $l_1 : l_2 : l_3$, we represent in fig. 7 the numbers of quantum states as a function of the total angular momentum J for all representative ratio $l_1 : l_2 : l_3$, corresponding to triangle AOD from Fig. 6. For each J value the number of states is divided by $2J+1$ in order to get the piecewise linear function [33]. The points of discontinuity of the first derivative of the number of state function correspond exactly to singular sections. From the physical point of view the number of states function shows simply the number of intermediate angular momentum values admissible for a given total angular momentum. Energy momentum map for the problem considered is three-dimensional because the problem has three degrees of freedom. But the additional degree of freedom which is related to the projection of the total angular momentum on the axis is in some sense unimportant due to symmetry. It can be simply considered as additional internal degree of freedom which is complitely uncoupled from the dynamical motion governed by two other degrees of freedom. To go from two-dimensional energy momentum map to three dimensional it is sufficient just to make the parallel transfer in the third (J_z) dimension taking into account the dependence of the range of J_z variation on J^2.

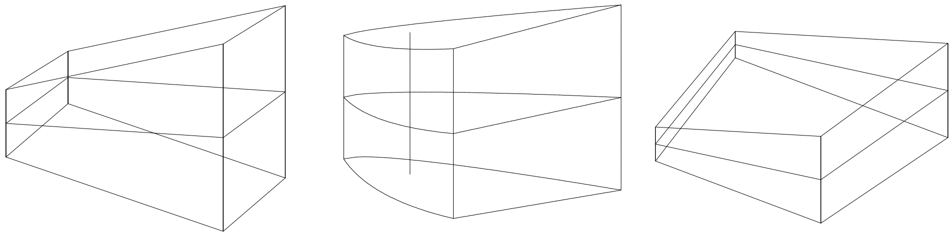

Fig. 8. Three dimensional energy-momentum map for one-parameter family of Hamiltonians. Central map shows the presence of monodromy line.

The schematic view of the energy momentum map for three different model Hamiltonians is given in Figure 8. Left and right figures correspond to the cases when singular points of the energy-momentum map are situated only on the boundary. In this case the action-angle variables are globally well defined inside the energy-momentum map. The central figure corresponds to the situation with a singular line surrounded by the regular values of the energy momentum map. At each $J_z = const$ slice (which cut the singular line) of the energy momentum map the isolated singular value results in the absence of global action-angle variables and in the presence of classical and quantum monodromy. It is possible to repeat here the same figure 2 just indicating that each point now corresponds to rotational band rather than to individual level. The degeneracy of bands is related with the second integral of motion value.

4 Perspectives

The relation between redistribution phenomenon and monodromy can be further extended to relation with topological quantum numbers which can be introduced to characterise energy bands [20,21]. Natural classification of bands by Chern classes of vector fibre bundles in the semi-quantum model was introduced recently [20,21] and it turns out that such topological description can be easily generalised to highly dimensional systems. Nevertheles, the interrelation between Chern classes in semi-quantum approach, quantum and classical monodromy, the density of quantum-states description, and classical Duistermaat-Heckman theorem [33–35] still remains to be pieces of unresolved puzzle.

References

[1] L. Michel, B. Zhilinskii. Symmetry, invariants, topology. I. Basic tools. Phys. Rep. **341**, 11-84 (2001)

[2] B. Zhilinskii. Symmetry, invariants, topology. II. Symmetry, invariants, topology in molecular models. Phys. Rep. **341**, 85-171 (2001).

[3] L. Michel, B. Zhilinskii. Symmetry, invariants, topology. III. Rydberg states of atoms and molecules. Basic group theoretical and toppological analysis. Phys. Rep. **341**, 173-264 (2001).

[4] B. Zhilinskii. Topological and symmetry features of intramolecular dynamics through high resolution molecular spectroscopy. Spectrochim Acta A, **52** 1471-1484 (1996).

[5] I. Pavlichenkov. Bifurcations in quantum rotational spectra. Phys. Rep. **226**, 175-279 (1993).

[6] W. Harter. Computer graphical and semiclassical approaches to molecular rotations and vibrations. Comput. Phys. Rep. **8**, 319-394 (1988).

[7] D.A. Sadovskii, B.I. Zhilinskii. Qualitative analysis of vibration-rotation hamiltonians for spherical top molecules. Mol. Phys. **65**, 109-128 (1988).

[8] I.M. Pavlichenkov, B.I. Zhilinskii. Critical phenomena in rotational spectra. Ann. Phys. (N.Y.) **184**, 1-32 (1988).

[9] D. Sadovskii, B. Zhilinskii, G. Pierre, J.P. Champion. Maniofestation of bifurcations and diabolic points in molecular energy spectra. J. Chem. Phys. **92**, 1523-1537 (1990).

[10] D. Sadovskii, B. Zhilinskii. Group-theoretical and topological analysis of localized rotation-vibration states. Phys. Rev. A **47**, 2653-2671 (1993).

[11] C. VanHecke, D. Sadovskii, B. Zhilinskii. Qualitative analysis of molecular rotation starting from inter-nuclear potential. Eur. Phys. J. D **7**, 199-209 (1999).

[12] B. Zhilinskii. Qualitative analysis of vibrational polyads: N mode case. Chem. Phys. **137**, 1-13 (1989).

[13] V. B. Pavlov-Verevkin, B. Zhilinskii. Rearrangement of vibrational polyads with excitation: two-mode case. Chem. Phys. **128**, 429-437 (1988).

[14] D. Sadovskii, B. Zhilinskii. Qualitative study of a model three-level Hamiltonian with $SU(3)$ dynamical symmetry. Phys. Rev. A **48**, 1035-10441 (1993).

[15] D. Sadovskii, N. Fulton, J. Tennyson, B. Zhilinskii. Nonlinear normal modes amd local bending vibrations of H_3^+ and D_3^+. J. Chem. Phys. **99**, 906-918 (1993).

[16] D. Sadovskii, B. Zhilinskii, L. Michel. Collapse of the Zeeman structure of the hydrogen atom in an external electric field. Phys. Rev. A **53**, 4064-4067 (1996).

[17] D. Sadovskii, B. Zhilinskii. Tuning the hydrogen atom in crossed field between the Zeeman and Stark limit. Phys. Rev. A **57**, 2867-2884 (1998).

[18] D. Sadovskii, B. Zhilinskii. Counting levels within vibrational polyads. Generating function approach. J. Chem. Phys. **103**, 10520-10536 (1995).

[19] B. I. Zhilinskii, M. I. El Idrissi, M. Herman. The vibrational energy pattern in acetyl;ene (VI): Inter and intrapolyad structures. J. Chem. Phys. **113**, 7885-7890 (2000).

[20] F. Faure, B. Zhilinskii. Topological Chern indices in molecular spectra. Phys. Rev. Lett. **85**, 960-963 (2000).

[21] F. Faure, B. Zhilinskii. Topological properties of the Born-Oppenheimer approximation and implications for the exact spectrum. Let. Math. Phys. in press.

[22] B. Fedosov. The Atiyah-Bott-Patodi method in deformation quantization. Comm. Math. Phys. **209**, 691-728 (2000).

[23] B. Fedosov. On G-Trace and G-Index in Deformation Quantization. Lett. Math. Phys. **52**, 29-49 (2000).

[24] V. B. Pavlov-Verevkin, D. Sadovskii, B. Zhilinskii. On the dynamical meaning of the diabolic points. Europhys. Lett. **6**, 573-578 (1987).

[25] R. Cushman, J. J. Duistermaat. The quantum mechanical spherical pendulum. Bull. Am. Math. Soc. **19**, 475 (1988).

[26] J. J. Duistermaat. On global action-angle variables. Comm. Pure Appl. Math. **33**, 687- (1980).

[27] L.M. Lerman, Ya. L. Umanskii. Four dimensional integrable Hamiltonian systems with simple singular points (topological aspects). Transl. Mathematical Monographs, **176**, AMS (1998).

[28] San Vu Ngoc, Quantum monodromy in integrable systems. Comm. Math. Phys. **203**, 465-479 (1999).

[29] D. Sadovskii, B. Zhilinskii. Monodromy, diabolic points and angular momentum coupling. Phys. Lett. A **256**, 235-244 (1999).

[30] R. Cushman, D. Sadovskii. Monodromy in the hydrogen atom in crossed fields. Physica D **142**, 166-196 (2000).

[31] L. Grondin, D. Sadovskii, B. Zhilinskii. Monodromy in systems with coupled angular momenta and rearrangement of bands in quantum spectra. (in preparation)

[32] H. Weyl, *Classical groups, their invariants and representations*, Princeton Univ., New Jersey. 1939

[33] J.J. Duistermaat, G. J. Heckman, On the variation in the cohomology of the symplectic form of the reduced phase space. Invent. Math. **69**, 259-269 (1982).

[34] V. Guillemin, Moment Maps and Combinatorial Invariants of Hamiltonian T^n-spaces. Birkhäuser, 1994, Ch. 2.

[35] M. Audin, The topology of Torus Actions on Symplectic Manifolds. Birkhäuser, 1991, Ch. 5.